Purdue University
Purdue e-Pubs

International Compressor Engineering Conference | School of Mechanical Engineering

2006

On the Structure of Compressor Gas Leakage Flows

Jan Prins
Danfoss A/S

Follow this and additional works at: http://docs.lib.purdue.edu/icec

Prins, Jan, "On the Structure of Compressor Gas Leakage Flows" (2006). *International Compressor Engineering Conference.* Paper 1728.
http://docs.lib.purdue.edu/icec/1728

This document has been made available through Purdue e-Pubs, a service of the Purdue University Libraries. Please contact epubs@purdue.edu for additional information.
Complete proceedings may be acquired in print and on CD-ROM directly from the Ray W. Herrick Laboratories at https://engineering.purdue.edu/Herrick/Events/orderlit.html

On the Structure of Compressor Gas Leakage Flow

Jan Prins
Danfoss Advanced Engineering
Nordborf 6430, Denmark
prins@danfoss.com

ABSTRACT

The understanding of leakage flows is considerably poor when one considers the large efficiency and capacity losses that leakage induces in compressors. An important reason for this is that few compressor engineers seem to comprehend the features of this type of flow that affect the mass flow rate. This paper presents a coherent qualitative picture of leakage flows that is consistent with experimental results. This picture is supported by the analysis of simple models.

1. INTRODUCTION

Compressor engineers are not especially interested in the details of leakage flows. In their eyes, the only relevant property is the mass flow rate, simply because that is the property that is directly related to the capacity and energy losses inside compressors. A useful definition of *the leakage flow problem* is therefore:

> Calculation of the mass flow rate given the pressure and temperature in the source, the pressure in the target, the geometry of the leakage path and the properties of the gas (see figure 1).

Unfortunately, this cannot be done without looking at flow in some detail. At an earlier occasion (Prins & Infante-Ferreira 1998) it was shown that one dimensional models fail to explain the effect of geometry on the flow rate as observed in experimental work by Peveling (1988), see figure 2. He established three geometry classes based on experiments including 27 differently shaped leakage gaps. Class **A** shows an almost constant value of the flow coefficient, classes **B** and **C** have considerably smaller and larger values respectively.

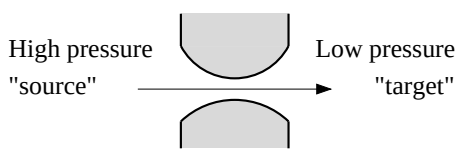

Figure 1: Typical leakage problem.

This paper intends to identify those structural features of leakage flows that affect the mass flow rate. For this, two highly idealized flow models are examined and the possibility of turbulence is discussed. The result is a coherent picture that can explain Peveling's results and that forms a solid starting point for the development of leakage models.

This paper does not aim for quantitative flow rate prediction. It only seeks for qualitative understanding that is needed for the design of quantitative models. Moreover, an engineer may have the freedom of designing the leakage gap geometry to minimize the associated losses. No attempts to do so have yet been found in literature.

This text will look at the application of simple models to the leakage flow problem. The underlying mathematics will not be discussed. The one dimensional models of section 2 are so elementary that they can be found in virtually every introduction text to fluid dynamics. References will be given for the two dimensional flow in section 3.

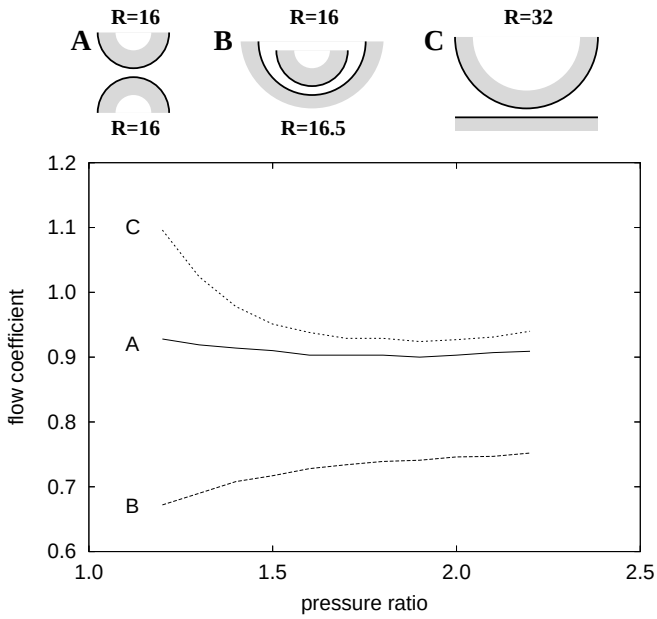

Figure 2: Flow coefficients for three examples of Peveling's geometry classes. (dimensions in mm, minimum gap 0.4 mm, compressed air exhausted into ambient)

2. ONE DIMENSIONAL FLOW

Much can be learned from one dimensional flow models. They do not provide all the answers, but they do give some reasonable ideas about what may be happening inside leakage gaps.

2.1 Isentropic Flow

The key assumption in isentropic flow is that the gas goes through an isentropic process while the conversion between enthalpy and kinetic energy is free of losses, thus:

$$s = \text{constant} \qquad \text{and} \qquad \Delta h = u^2/2 \tag{1}$$

Here s is the entropy, h is the enthalpy and u is the velocity of the gas. Figure 3 shows that this makes it possible to read the velocity as a function of the pressure from a thermodynamic chart, provided that the condition in the source is given.

A more detailed chart also provides the density (or the specific volume). Multiplied by the velocity, this gives the flow per unit area, as shown in figure 4. It shows a very important feature: there is a maximum to the flow rate per unit area, the so called critical point. This is a common feature of compressible flow models. In this particular model, it occurs at the speed of sound.

Now consider a given mass flow rate through a converging-diverging nozzles such as shown in figure 2. The flow rate per unit area increases as the flow area decreases. The condition of the gas slides down the isentropic line in figure 3 while it converts its enthalpy into kinetic energy. Beyond the throat, the area increases again and the gas reverses its decent. Since the velocity in the source and the target are negligible, the gas returns to its original point in the chart. A range of these subsonic solutions is shown in figure 5. They all predict that the target pressure equals the source pressure. This is obviously conflicting with the original leakage flow problem as formulated above.

When the mass flow rate is such that it reaches the critical point in the throat, another solution appears. The flow rate per unit area may now decrease by further acceleration. The density drops so fast that it over-compensates the increasing velocity. Instead of reversing the process in figure 3, the gas simply continues to

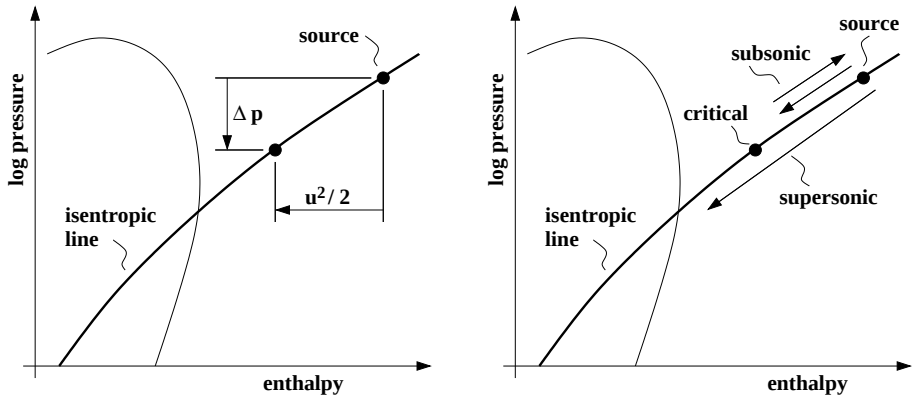

Figure 3: The one dimensional isentropic flow model depicted in the log PH diagram. The left shows the relation between pressure, enthalpy and velocity. The right depicts subsonic and supersonic flows.

expand. This is the supersonic solution (see figure 5). Note that this solution is only possible for one specific flow rate. The phenomenum is known as choking. Again, it does not allow for an arbitrary pressure in the target.

Although we obtained two different solutions for the flow, neither of them solves our problem. We want to prescribe the target pressure but it is not a free parameter in the isentropic flow model. Some non-isentropic features need to be introduced to obtain a workable model.

2.2. Isentropic-Isobaric Flow

A simple modification assumes that the flow becomes isobaric at some point in the diverging part of the gap. This obviously allows arbitrary target pressures but introduces the problem of determining the transition point. Figure 6 shows the pressure distributions for some solutions with the same source and target pressures but different choices for the transition point. The throat pressures are all different and therefore, the flow rates are also quite different. As the transition point moves downstream, the flow rate increases.

The only point that suggests itself for the transition is the throat. This assumption is made in *the* isentropic model that is used to define the flow coefficient. Its name is somewhat incorrect because it actually assumes an isobaric part of the flow rather than a fully isentropic flow. When the transition point lies downstream of throat, the flow will be larger than the reference and the flow coefficient will be larger than one.

This modification to the isentropic model describes the behaviors of the class **A** and class **C** geometries in figure 3. The first becomes isobaric in the throat area and the flow rate is close to the reference value: the flow coefficient is roughly constant and close to one. The class **C** geometry recovers more of the pressure drop in the diverging part of the gap and exhibits a correspondingly larger flow rate. However, it does not yet explain what determines the pressure recovery. This will be discusses in section 3.

2.3. Normal shock waves

Normal shock waves allow for arbitrary outlet pressure in a supersonic solution of the isentropic flow model. These shocks are not reversible and therefore add non-isentropic features to the model.

In a normal shock, a supersonic flow jumps to a subsonic flow on a sub-micrometer scale. The pressure, density and temperature increase almost instantaneously while the velocity decreases. The strength of the shock is solely determined by the pre-shock Mach number, thus by the position inside the gap where it appears.

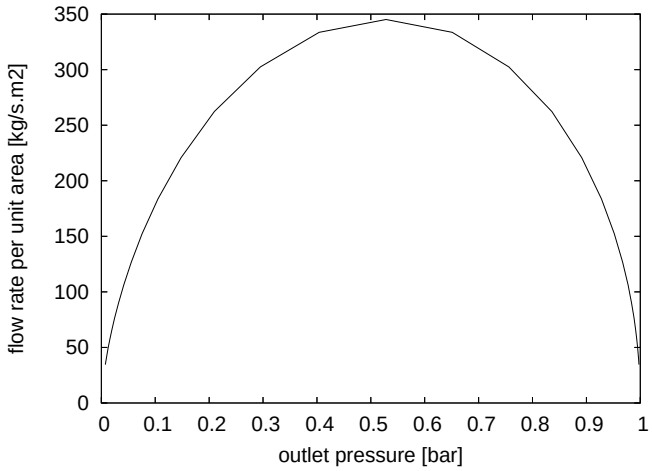

Figure 4: Mass flow rate per unit area as a function of the outlet pressure. This figure is made for ambient air at the inlet.

Figure 7 shows supersonic solutions with the same inlet condition but different target pressures. As the outlet pressure approaches the source pressure, the shock is found close to the throat. Note that this leads to supersonic solutions even when the pressure ratio is almost equal to one. Comparison with figure 6 shows that two solutions have now been found for pressure ratios between one and the critical value: an isobaric-isentropic solution and a supersonic solution with a shock wave. Only the supersonic solution with a shock exists for target pressures below the critical value.

3. TWO DIMENSIONAL FLOW

One dimensional flow does not explain why or where the flow changes from isentropic to isobaric. This picture is also a strong simplification. But somehow, the truth must be in between the total pressure recovery of isentropic flow and the absence of pressure recovery in the isobaric flow. Further understanding requires insights into the multi-dimensional features of the flow.

This section looks at the incompressible flow between two infinite flat plates. It is one of the few two dimensional flows for which an exact solution exists. It will be assumed that the same flow patterns are found as in compressible flow. The solution is due to Jeffery (1915a,1915b) and Hamel and bears their names. Concise explanations can be found in Schlichting and Gersten (2003) and White (1974). Due to the limited space available for this paper, the discussion here will be kept to a minimum, only indicating the broad view.

3.1. Converging Flow

The solution of converging Jeffery-Hamel flow is sketched in figure 8. It shows a strong boundary layer character with a uniform profile in the center and a steep decline towards zero velocity in thin regions near the walls. The boundary layer thickness decreases with increasing opening angle between the walls.

The wall friction is, according to Newton's law for the shear stress, proportional to the velocity gradient at the wall. As a result of the boundary layer character, this gradient is large and the wall shear stress will be high. The boundary layer thickness decreases when the opening angle of the walls decreases, giving a tendency towards high wall friction. On the other hand, the region of small flow area, and therefore high velocity, decreases with the opening angle. This gives a tendency towards low wall friction. Quantitative analysis of the Jeffery-Hamel flow shows that the second effect is the stronger of the two. Thus small opening angles give the maximum friction losses in the flow. As friction reduced the mass flow rate, this is a useful feature for compressor engineers.

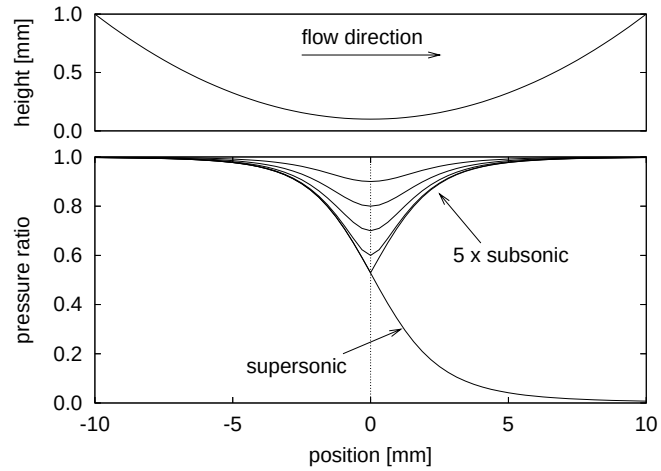

Figure 5: Pressure distributions of five subsonic solutions and the only supersonic solution.

3.2. Diverging Flow

The shape of the velocity profile in diverging flows shows much more variation than in converging flows, as sketched in figure 9. For low opening angles and low velocity, the profile is similar to that of converging flow, but, the boundary layer character has vanished. The profile is much more rounded.

As the opening angle and/or velocity increase, the profile first start to deflect and finally a region of reversed flow occurs at the wall. The latter is known as viscous separation. It can be explained from the interaction of pressure forces and shear forces within the flow.

The result of separation is that the effective area of the flow decreases. The apparent opening angle seems to be smaller than it is in reality. The velocity will therefore be higher and the conversion from momentum into pressure (or kinetic energy into enthalpy) is less effective. The net result is less pressure recovery and less mass flow rate. A large opening angle is therefore reducing leakage losses.

Another form of separation occurs when the wall curves sharply outwards. This effect is much like a train running out the rails when it enter a curve too fast. It also suppresses pressure recovery. This is known as massive wall separation (see figure 10).

4. DISCUSSIONS AND CONCLUSIONS

The analysis above reveals two flow features that are related to the gap's geometry and that dominate the leakage flow rate:

- Friction is dominant in the converging part of the gap. In order to maximize its effect, this part of the gap should be long and narrow.
- At low pressure ratios, the pressure recovery in the diverging part of the flow induces the flow rate. This negative effect is suppressed by a large opening angle or a sharp outward curve in the wall.

This suggests the addition of a fourth geometry class as shown in table 1. It could not have been found by Peveling because he only used symmetric gap (converging and diverging parts are each others mirror images). A high friction geometry has therefore also a high pressure recovery.
No reports about employing these insights into a compressor design have been found in literature. In some compressor types, this is a possibility. Consider for example the gap between a screw rotor tip and the housing. Figure 11 shows a four examples. The class **D** geometry represents the smallest leakage, class **C** the highest.

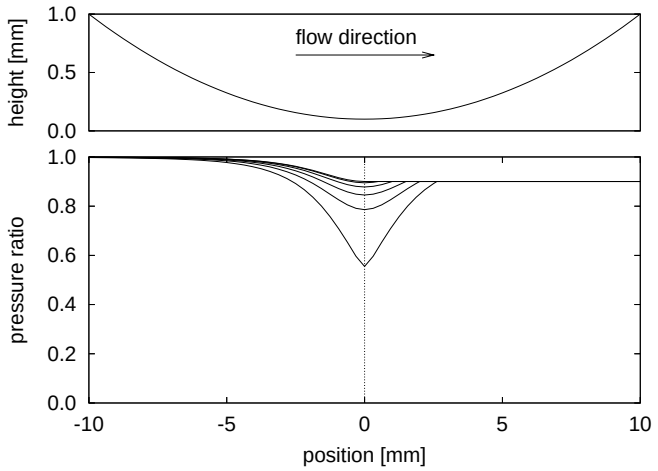

Figure 6: Isentropic-isobaric solutions for the same source and target conditions but with different choices for the transition point.

	low pressure recovery	high pressure recovery
low friction	class **A**	class **C**
high friction	class **D**	class **B**

Table 1: The four geometry classes that are suggested by the analysis in this paper. Class **D** has been added to the three earlier identified by Peveling.

REFERENCES

Jeffery G.B., 1915a, The equations of motion of a viscous fluid, *Philosophical Magazine and Journal of Science*, pp. 445-454

Jeffery G.B., 1915b, The two-dimensional steady motion of a viscous fluid, *Philosophical Magazine and Journal of Science*, pp. 455-465

Peveling F.J., 1988, Ein Beitrag zur optimierung adiabater Schraubenmaschinen in Simulationsrechnungen, *VDI-Fortschritt Berichte, Reihe 7, Nr. 135, VDI-Verlag*, Düsseldorf

Prins J., Infante-Ferreira C.A., 1998, Quasi one-dimensional steady-state models for gas leakage, parts I & II, *Proc. Compressor Eng. Conf. at Purdue*, pp. 571-582

Schlichting H., Gersten K., 2003, Boundary layer theory, *Springer, Berlin*, Corrected 8th edition, sec. 5.1.2

White F.M., 1974, Viscous fluid flow, *McGraw-Hill, New York*, sec. 3-8.7

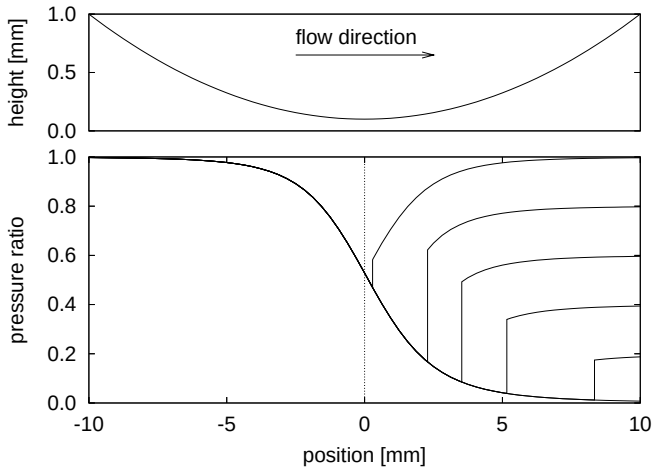

Figure 7: Supersonic solutions with normal shock waves. The target pressure determines the position of the shock inside the gap.

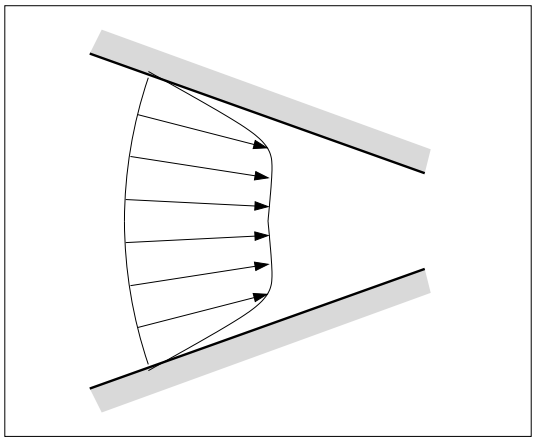

Figure 8: Sketch of the velocity profile in a converging flow according to the Jeffery-Hamel solution.

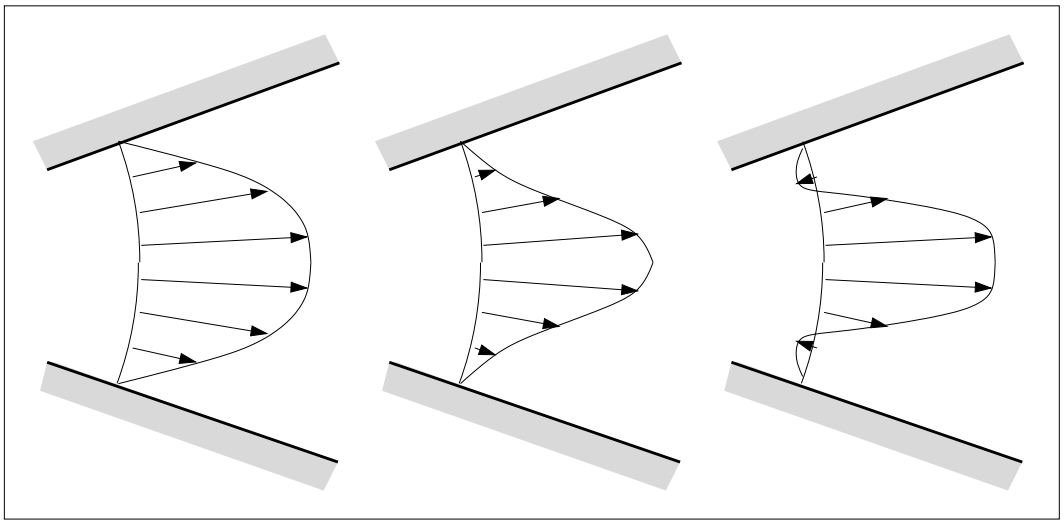

Figure 9: Sketch of the different shapes of the velocity profiles in a diverging flow according to the Jeffery-Hamel solution.

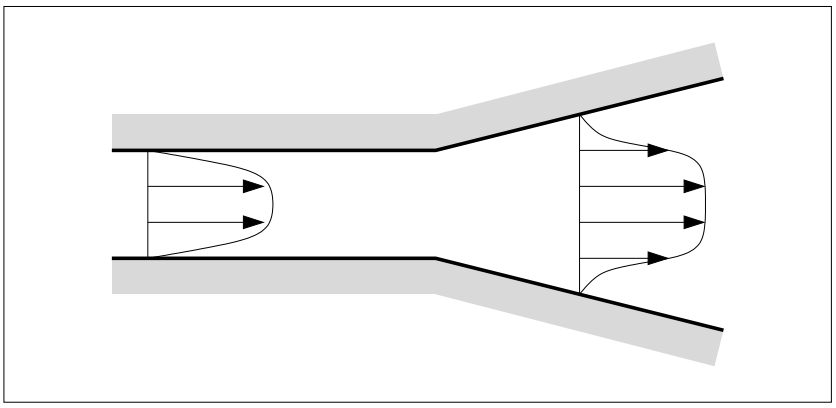

Figure 10: Sketch of massive wall separation.

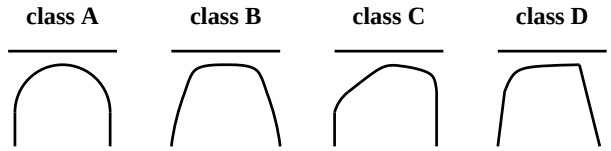

Figure 11: Rough sketch to illustrate how a screw rotor tip design affects the flow rate through the house sealing line. The flow is directed left-to-right.